Experimental Evidence of Threshold Effects in the Energy Loss of Protons in Carbon and Aluminum due to Inner Shell Ionization

M. Famá, J. C. Eckardt, G. H. Lantschner, and N. R. Arista

Instituto Balseiro and Centro Atómico Bariloche, Comisión Nacional de Energía Atómica, RA-8400 S.C. Bariloche, Argentina

(Received 15 May 2000)

We explore the contributions of inner shell ionization to the energy loss of 7 to 270 keV protons in C and Al foils under experimental conditions such that the product of the observation angle and the projectile energy is kept constant. By normalizing these energy loss measurements to the energy loss in the forward direction we observe a pronounced rising behavior with increasing energy. This effect appears in the same range of energies where the respective K- and L-shell ionization cross sections of these elements show a similar threshold behavior. Based also on various theoretical considerations we interpret these results as clear evidence of the inner shell ionization contribution to the energy loss.

PACS numbers: 34.50.Bw, 34.50.Fa

It is well known that the electronic energy loss of slow ions in solids (with velocities below the Bohr velocity) is due to the interaction with conduction or valence electrons of the medium, whereas with increasing velocities the mechanism of inner shell ionization becomes increasingly important [1]. Based on this knowledge one may expect that with increasing energies some evidence of the thresholds for the ionization of the various inner shells would be observed. In fact, the phenomenon of inner shell ionization by swift protons has been studied extensively using x-ray spectroscopy techniques, and in particular the processes of K- and L-shell ionization by light ions are well described by the standard theories [2–8].

However, a direct evidence of threshold effects in the contribution of inner shells to the total energy loss of swift ions in solids has so far not been observed, and the reason for this is simply that these effects are usually masked in the standard measurements of total energy losses, or stopping powers, due to an average over a multitude of electronic excitation processes; so that, at the end, a smooth stopping function corresponding to the envelope of these many processes is observed. For instance, an estimation of the L-shell contribution to the total energy loss of protons in aluminum using the harmonic oscillator model [9] yields a rise from 1% at 20 keV to 16% at 100 keV. In the same energy range, the Al L-shell ionization cross section increases by an order of magnitude [8].

In this respect, it is also interesting to note that rather small threshold effects (due to the excitation of *outer* shells) have been observed for slow ions in certain materials, which are related to particular effects in the band structure of some metals [10] (deviations from a free electron behavior) or in wide band gap insulators [11]. But the observation of similar effects at higher energies due to inner shell ionization has so far not been achieved for the reasons already indicated.

We propose here a different experimental approach to study the contribution of inner shells to the energy loss of ions in solids, which is based on the enhancement of that contribution with increasing observation angles, in beam foil transmission experiments.

Here we provide direct experimental evidence of threshold effects due to inner shell ionization in the energy loss of protons in solids from energy loss measurements performed under special experimental conditions. We have performed transmission experiments using thin foils, varying the energy E of the ion beam and simultaneously changing the observation angle θ, while keeping constant the product θE. Normalizing the energy loss measurements $\Delta E(\theta)$ to the energy loss in the forward direction, $\Delta E(\theta = 0)$, the effect of small impact parameter collisions is magnified and so we observe the appearance of threshold effects in the energy loss of swift protons in C and Al, which are due to the ionization of the K and L shells, respectively. The energy threshold for both elements appears in the range of energies where the ionization cross sections (K shell for C and L shell for Al) show a similar threshold behavior. The normalization used also makes the results independent of foil inhomogeneities as will be discussed below. These inhomogeneities would otherwise mask the threshold effect.

The experimental procedure is based on the so-called *scaling principle* [12] where the quantity θE in small-angle forward scattering is primarily a function of the impact parameter b. This can also be expressed in terms of the differential scattering cross section parametrized in the usual way [13] as $d\sigma = \pi a^2 t^{-1} f(t^{1/2}) d(t^{1/2})$, where $t^{1/2} \simeq a\theta E/(2Z_1 Z_2 e^2)$ in the small angle approximation, with a the screening radius, e the elementary charge, Z_1 and Z_2 the atomic numbers of the ion and target, respectively. According to this, under single-collision conditions, it is possible to study the interactions between projectile and target at constant impact parameter, by varying simultaneously the projectile energy E and the observation angle θ, with $\theta E =$ constant. Because of the multiple scattering phenomena, single-collision conditions cannot be obtained in solids. Nevertheless, from Ref. [14] one can see that the multiple scattering function $F(x, \theta)$, describing the angular

 0031-9007/00/85(21)/4486(4)$15.00

distribution of a particle beam after traversing a thin layer of thickness x, can be written as well in terms of reduced units as follows:

$$F(x,\theta) \equiv f(\tau,\tilde{\theta}), \tag{1}$$

where $\tau = \pi a^2 N x$, $\tilde{\theta} = t^{1/2} = a\theta E/(2Z_1 Z_2 e^2)$, and N is the target atomic density. From the reduced angle expression we see that the multiple scattering function preserves the scaling property, so that it remains unchanged when it is evaluated keeping the product θE constant.

A projectile that exits the foil with an observation angle θ, has suffered a certain number of collisions inside the foil, with different scattering angles ψ. The corresponding differential scattering angle distribution may be expressed in reduced units as [15]

$$d\eta(\tau,\tilde{\theta},\tilde{\psi}) = \frac{\tau}{\pi a^2}\,\frac{d\sigma(\tilde{\psi})}{f(\tau,\tilde{\theta})}\int_0^{2\pi} f(\tau,|\tilde{\boldsymbol{\theta}} - \tilde{\boldsymbol{\psi}}|)\,\frac{d\tilde{\alpha}}{2\pi}, \tag{2}$$

where bold symbols denote vectors in a plane perpendicular to the incident beam direction (small angle approximation), $d\sigma(\tilde{\psi})$ is the differential scattering cross section which has the scale property mentioned above, and $\tilde{\alpha}$ is the angle between $\tilde{\boldsymbol{\theta}}$ and $\tilde{\boldsymbol{\psi}}$. Because of the scaling principle, $\tilde{\psi} \propto \psi E$ represents a given impact parameter b. Therefore, when observing the transmitted energy spectra in conditions where $\tilde{\theta} \propto \theta E =$ constant, we are considering a fixed distribution of impact parameters inside the target foil.

The energy losses were measured using the transmission method with very thin smooth foils ($\sim$20 nm). Here, only a short description of the experiment is given; more details can be found in Refs. [16,17]. To cover the present energy range, two ion accelerators were used. Protons with $E < 10$ keV were generated by a hot discharge ion source followed by focusing and accelerating stages, a Wien filter for mass selection, and a 18° electrostatic deflector to get rid of neutral particles. Energy losses as a function of the observation angles were measured with a 127° rotatable electrostatic energy analyzer, with a precision of ± 10 eV, and an angular resolution of $\pm 0.58°$. The higher energy region ($15 < E < 270$ keV) was covered with protons generated by a Cockroft-Walton electrostatic accelerator with a rf ion source and a magnetic mass selection. In this case the observation angle is selected by electrostatic deflection of the emerging ions. This method, especially suited for small angles, has the advantage that a fixed plate potential corresponds to a constant θE value. In this case the precision of the energy loss determinations was ± 15 eV, and the angular resolution was $\pm 0.05°$.

These experiments were performed by simultaneous variations of the beam energy E and observation angle θ such that the product θE remained constant at 100 keV-deg.

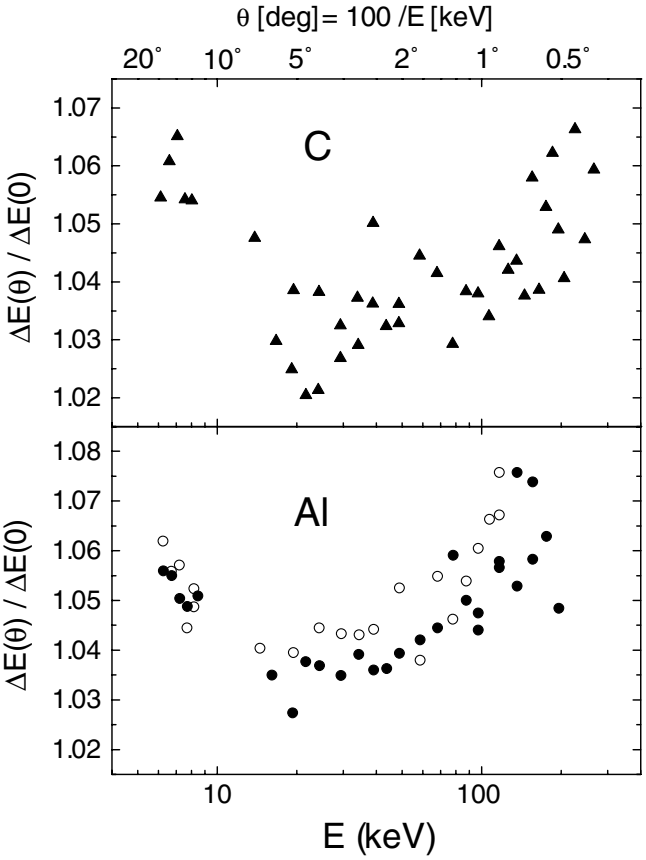

FIG. 1. Normalized energy loss as a function of projectile energy for protons observed at $\theta[\text{deg}] = 100/E[\text{keV}]$ transmitted in a thin C foil (23 nm) and two Al foils (21 nm). Solid and open circles for aluminum correspond to the different foils.

In Fig. 1 we present experimental results of the normalized energy loss $\Delta E(\theta,E)/\Delta E(0,E)$ for one carbon foil (23 nm) and two aluminum foils (21 nm) as a function of proton energy for a constant θE value. We note that this ratio increases both at low and at high energies.

In a recent publication [17] comparing Monte Carlo simulations with experimental results it was shown that in the very low energy range ($E < 10$ keV) the angular dependence of the energy loss for protons traversing thin metal foils can be fully explained considering the contribution to the mean energy loss of the following three factors: foil roughness effect, path length enlargement, and elastic energy loss, i.e., $\Delta E(\theta,E) = \overline{\Delta E} + \Delta E(\theta,E)_{\text{roughness}} + \Delta E(\theta,E)_{\text{path enl.}} + \Delta E(\theta,E)_{\text{elastic}}$. The last two become important for observation angles $\theta \gtrsim 5°$. The effect of foil roughness on the mean energy loss in the normalized representation becomes constant (in conditions of θE constant) since it may be expressed in terms of reduced variables as follows [18]:

$$\frac{\overline{\Delta E} + \Delta E(\theta,E)_{\text{roughness}}}{\Delta E(0,E)} = \frac{1 + \rho^2\partial \ln f(\tau,\tilde{\theta})/\partial \ln\tau}{1 + \rho^2\partial \ln f(\tau,0)/\partial \ln\tau} = 1 + c\,, \tag{3}$$

where ρ is the roughness coefficient and c depends on ρ, τ, and $\tilde{\theta}$, but remains constant under the present experimental conditions. This independence of the foil roughness effect is the main reason for the present normalization method. As a consequence of these considerations it may be shown that the increase of $\Delta E(\theta, E)/\Delta E(0, E)$ observed in Fig. 1 for decreasing energies is essentially due to path length enlargement and elastic energy loss effects. These two effects become negligible at higher energies, since $\theta[\text{deg}] = 100/E[\text{keV}]$ becomes very small. Nevertheless, one can observe in Fig. 1 a remarkable increase of $\Delta E(\theta, E)/\Delta E(0, E)$ with E in this energy region, for both targets. This indicates that there are additional inelastic effects on the energy loss $\Delta E(\theta, E)$ which are not included in the previous equations. We show below that this additional contribution is the inelastic term expected from inner shell ionization to be called $\Delta E(\theta, E)_{\text{inelastic}}$. Taking into account the scattering angle distribution of Eq. (2) and assuming an inelastic energy loss per collision $Q(E, \tilde{\psi})$, the total contribution of the observable inelastic term is given in terms of the present variables by [15]

$$\Delta E(\theta, E)_{\text{inelastic}} = \int d\eta(\tau, \tilde{\theta}, \tilde{\psi}) Q(E, \tilde{\psi}). \quad (4)$$

To isolate the effect of this inelastic term we subtract from the total energy loss $\Delta E(\theta, E)$ the contributions from path length enlargement and elastic energy loss, as described in Ref. [17], obtaining the quantity $\Delta E^*(\theta, E) = \Delta E(\theta, E) - \Delta E(\theta, E)_{\text{path enl.}} - \Delta E(\theta, E)_{\text{elastic}}$, which we normalize with respect to the $\Delta E(0, E)$ value. Thus we obtain

$$\frac{\Delta E(\theta, E)^*}{\Delta E(0, E)} = 1 + c + \frac{\Delta E(\theta, E)_{\text{inelastic}}}{\Delta E(0, E)}. \quad (5)$$

In Figs. 2 and 3 we show a fit of $1/\Delta E(0, E)$ from the present measurements, together with the energy dependence of the ionization cross sections of the carbon K shell and the aluminum L shell [7,8] and the experimental results from Fig. 1 in the form $\Delta E(\theta, E)^*/\Delta E(0, E) - 1$. This expression equals $c + \Delta E(\theta, E)_{\text{inelastic}}/\Delta E(0, E)$ from Eq. (5). The constancy observable at low energies, in spite of the large amplification introduced by the $1/\Delta E(0, E)$ factor, corresponds to the constant roughness effect mentioned above. It indicates that there is no influence of additional inelastic mechanisms on the energy loss in this region. The relative displacement of the two sets of data points for aluminum corresponds to different values of the c constant arising from differences in the roughnesses of the two foils.

The most interesting feature that we want to note in both Figs. 2 and 3, is the remarkable increment of the additional energy loss contribution at high energies. This behavior is quite similar to the energy dependence of the K and L shell ionization cross sections for carbon and aluminum, respectively, shown in the upper panels of the figures.

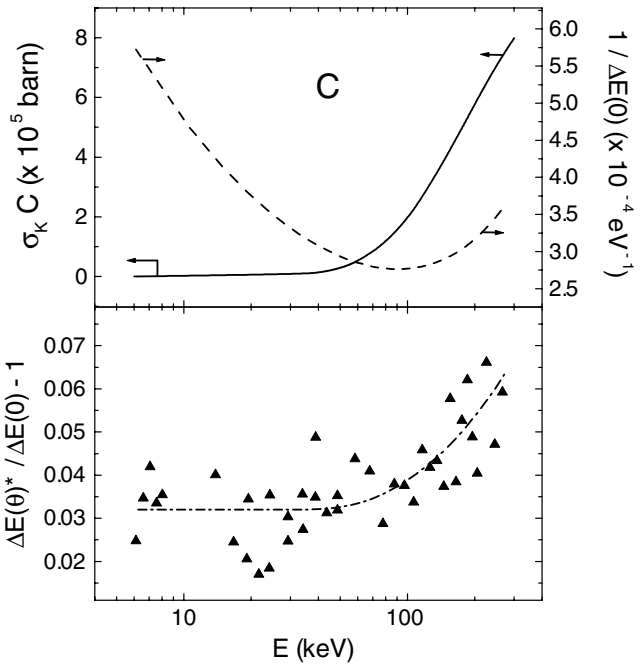

FIG. 2. Top: (- - - -) Fitted expression for $1/\Delta E(0, E)$ taken from the present measurements in C. (——) Cross section for K-shell ionization by protons [7]. Bottom: Experimental data from Fig. 1, subtracting path enlargement and elastic energy loss contributions. The constancy observed at low energies indicates a negligible contribution of inelastic terms (see text). The dash-dotted line shows the theoretical model.

To estimate the inelastic energy loss due to i-shell ionization according to Eq. (4), we used the harmonic oscillator model to calculate the stopping number $L_i[n_i(\mathbf{r}), v]$ for this shell [9], which, together with a local density approximation [19], give the energy loss per collision $Q_i(b)$ as follows:

$$Q_i(b) = \int dl \left(\frac{dE}{dx}\right)_i = \frac{4\pi Z_2^2 e^4}{m v^2} \int dl\, n_i(\mathbf{r}) L_i[n_i(\mathbf{r}), v], \quad (6)$$

where $n_i(\mathbf{r})$ corresponds to the electronic density of the i shell obtained from Hartree-Fock calculations. The integration was simplified by considering a straight line trajectory with an effective impact parameter b_{eff} for the inelastic processes. The results of these calculations are shown in Figs. 2 and 3 together with the experimental points. To make this comparison, we divided the theoretical values by the fitted $\Delta E(0, E)$ values obtained in this experiment and included a constant term c, as indicated in Eq. (5). In the case of aluminum we obtain two lines due to the different c values, arising from the different foil roughnesses. A good agreement with the experimental data was obtained from these calculations using $b_{\text{eff-C}} = 0.1$ a.u., $b_{\text{eff-Al}} = 0.4$ a.u., for carbon and aluminum, respectively. These values are smaller than the corresponding shell radii, as expected in a semiclassical picture of ionization processes produced by ions that penetrate the corresponding shells. However, we note that these

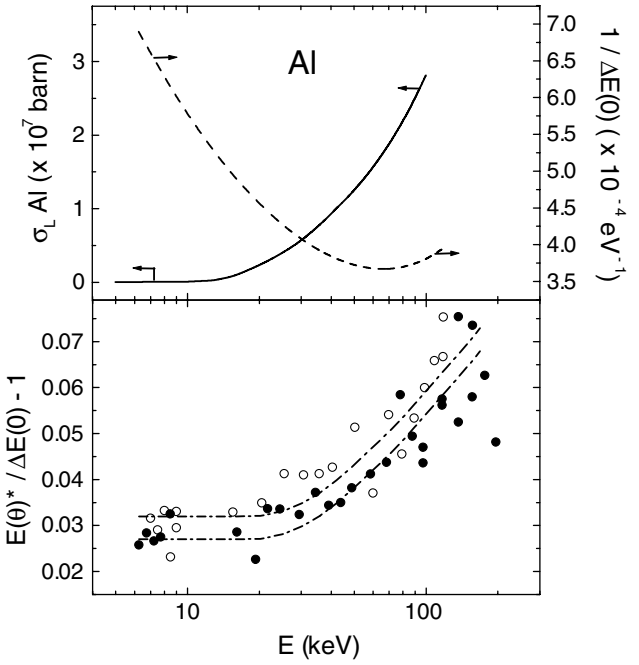

FIG. 3. Top: (- - - -) Fitted expression for $1/\Delta E(0, E)$ taken from the present measurements in Al. (——) Cross section for L-shell ionization by protons [8]. Bottom: Experimental data from Fig. 1, subtracting path enlargement and elastic energy loss contributions. The constancy observed at low energies indicates a negligible contribution of inelastic terms, and the observed differences in height between both foils are due to different roughnesses (see text). The dash-dotted lines show the theoretical model.

calculations may be improved by more precise impact-parameter formulations (a question that lies outside the scope of this Letter).

In addition, we note that the binding energies of the $2s$ and $2p$ L-shell electrons of aluminum are ~120 and ~80 eV, respectively, whereas the corresponding value for the K-shell electrons of carbon is ~290 eV. This significant difference in binding energies is considered to be the reason for the shift of the proton energies corresponding to the appearance of the threshold behavior observed in Figs. 2 and 3. It may be observed that the oxygen present in the oxide layers on the aluminum-foil surfaces does not affect the threshold effect because of the great difference in the binding energy of the oxygen K shell (~540 eV).

The present results provide a direct experimental evidence of a threshold effect in the energy loss of protons due to inner shell ionization phenomena. We have shown that a combined study of the energy and angular dependences of proton energy losses in an extended energy range, based on the small-angle scaling properties of single and multiple scattering processes (in terms of the θE parameter) provides valuable information on the energy loss phenomenon, which cannot be obtained from the usual stopping power experiments. This information may be useful to test the models on the impact parameter dependence of the energy loss due to inner shell ionization, as well as to improve the numerical simulations of ion transport in matter by a more precise description of the energy loss mechanisms.

Acknowledgment is made to R. Baragiola, H. Ascolani, and G. Zampieri for valuable suggestions and discussions. This work was supported in part by the Argentine Consejo Nacional de Investigaciones Científicas y Técnicas (Project No. PIP 4267) and the Agencia Nacional de Promoción Científica y Tecnológica (Project No. PICT0303579). One of us, M. F., thanks the FOMEC program.

[1] M. A. Kumakhov and F. F. Komarov, *Energy Loss and Ion Ranges in Solids* (Gordon and Breach Science Publishers, Inc., New York, 1981).
[2] G. Basbas, W. Brandt, and R. Laubert, Phys. Rev. A **7**, 983 (1973).
[3] G. Basbas, W. Brandt, and R. Laubert, Phys. Rev. A **17**, 1655 (1978).
[4] W. Brandt, At. Phys. **3**, 155 (1973).
[5] W. Brandt and G. Lapicki, Phys. Rev. A **20**, 465 (1979).
[6] W. Brandt and G. Lapicki, Phys. Rev. A **23**, 1717 (1981).
[7] H. Paul and J. Sacher, At. Data Nucl. Data Tables **42**, 105 (1989).
[8] C. Benazeth, M. Hou, N. Benazeth, and C. Mayoral, Nucl. Instrum. Methods Phys. Res., Sect. B **33**, 295 (1988).
[9] P. Sigmund and U. Haagerup, Phys. Rev. A **34**, 892 (1986); H. H. Mikkelsen and P. Sigmund, Nucl. Instrum. Methods Phys. Res., Sect. B **27**, 266 (1987); H. H. Mikkelsen and P. Sigmund, Phys. Rev. A **40**, 101 (1989).
[10] J. E. Valdés, J. C. Eckardt, G. H. Lantschner, and N. R. Arista, Phys. Rev. A **49**, 1083 (1994).
[11] C. Auth, A. Mertens, H. Winter, and A. Borisov, Phys. Rev. Lett. **81**, 4831 (1998).
[12] F. T. Smith, R. P. Marchi, W. Aberth, D. C. Lorents, and O. Heinz, Phys. Rev. **161**, 31 (1967).
[13] J. Lindhard, V. Nielsen, and M. Scharff, Mat. Fys. Medd. Dan. Vidensk. Selsk. **36**, 10 (1968).
[14] P. Sigmund and K. B. Winterbon, Nucl. Instrum. Methods **119**, 541 (1974).
[15] M. M. Jakas, G. H. Lantschner, J. C. Eckardt, and V. H. Ponce, Phys. Rev. A **29**, 1838 (1984).
[16] J. C. Eckardt, G. H. Lantschner, M. M. Jakas, and V. H. Ponce, Nucl. Instrum. Methods Phys. Res., Sect. B **2**, 168 (1984).
[17] M. Famá, G. H. Lantschner, J. C. Eckardt, C. D. Denton, and N. R. Arista, Nucl. Instrum. Methods Phys. Res., Sect. B **164–165**, 241 (2000).
[18] M. M. Jakas and N. E. Capuj, Nucl. Instrum. Methods Phys. Res., Sect. B **36**, 491 (1989).
[19] V. V. Balashov, *Interaction of Particles and Radiation with Matter* (Springer-Verlag, Berlin, 1993).